



# Corrosion behavior of Cr-based bulk metallic glasses in hydrochloric acid solutions



J.J. Si, X.H. Chen, Y.H. Cai, Y.D. Wu, T. Wang, X.H. Hui\*

State Key Laboratory for Advanced Metals and Materials, University of Science and Technology Beijing, Beijing 100083, China

## ARTICLE INFO

### Article history:

Received 16 September 2015

Received in revised form 14 February 2016

Accepted 15 February 2016

Available online 18 February 2016

### Keywords:

A. Acid solutions

A. Alloy

B. Polarization

B. XPS

C. Acid corrosion

C. Amorphous structures

## ABSTRACT

The corrosion behavior of  $\text{Cr}_{40}\text{Co}_{39}\text{Nb}_7\text{B}_{14}$  and  $\text{Cr}_{50}\text{Co}_{29}\text{Nb}_7\text{B}_{14}$  bulk metallic glasses in HCl solutions were investigated by immersion, electrochemical tests and microstructural observation. XPS analyses were performed to clarify chemical states of elements in the passive films. The results show that these alloys can be passive against corrosion in 1 and 3 M HCl, and high Cr content in the alloys has advantages on passivation properties. Increasing the exposure time in air and immersion time in 3 M HCl can accelerate the passivation. The high corrosion resistance is attributed to the highly-enriched trivalent Cr-oxide films formed in corrosive environments.

© 2016 Elsevier Ltd. All rights reserved.

## 1. Introduction

Unlike the traditional crystalline materials with defects such as grain boundaries and micro-structural heterogeneity, metallic glasses (MGs) with corrosion-resistant components were expected to possess superior corrosion resistance to their crystalline counterparts [1–8] owing to the homogeneous monolithic nature in the composition and structure in long range scale [9–11].

In Zr-[5,9,10], Ti-[11,12], Fe-[1–3,13,14], Ni-[6,15], Cu-[4,16], and Al-based [17,18] MG systems, numerous MGs with high corrosion resistance have been reported. The superior corrosion resistance properties of most MGs were attributed to the formation of homogeneous and protective oxide films. Especially, it has been widely found [13–15,19–25] that the alloying element Cr plays a critical role in improving corrosion resistance of Fe- and Ni-based MG, which are promising to be used in corrosion-resistant coating industry [26–28].

As early as 1974, it was reported [13] that  $\text{Fe}_{80}\text{Cr}_{10}\text{P}_{13}\text{C}_7$  glassy ribbon was corrosion free in 1 M HCl, while crystalline 304 stainless steel was severely corroded in the same solution. Since then, the role of Cr in many MG systems has been extensively investigated [29,30], and a variety of Fe-, Co- and Ni-based glassy alloys containing Cr have been developed [2,3,31–33]. In the early of this

century, corrosion-resistant Fe-Cr-Mo-C-B bulk metallic glasses (BMGs) with high Cr content were developed by Pang et al. [34,35], and it was found the  $\text{Fe}_{42}\text{Cr}_{16}\text{Mo}_{16}\text{C}_{18}\text{B}_8$  BMG exhibited high corrosion resistance even in concentrated hydrochloric acid. Pang et al. [36] also found that the addition of P into Fe-Cr-Mo-C-B BMGs further improved the corrosion resistance. Owing to the positive effect of minor addition of rare earth element Y, Fe-Cr-Mo-C-B-Y BMGs could show much higher glass forming ability (GFA) [37]. However, Shan [38] and Gostin et al. [39] found that the  $\text{Y}_2\text{O}_3$  particles formed in casting process were harmful to the corrosion resistance of these BMGs. Na et al. [40,41] developed a  $\text{Ni}_{68.6}\text{Cr}_{8.7}\text{Nb}_3\text{P}_{16}\text{B}_{3.2}\text{Si}_{0.5}$  BMG, which showed critical dimension of over one centimeter and low corrosion rate of less than  $10^{-2}$  mm/year in 6 M HCl at room temperature. To sum up, it can be found that the studies in Cr-bearing BMGs were almost focused on Fe-Cr-Mo-C-B(Y) and Ni-Cr-Nb-P-B BMG systems.

The superb corrosion resistance of the reported Cr-bearing MGs has been primarily attributed to the formation of protective Cr-rich oxide films [19–22,34,35], although all the constituent elements may affect the corrosion resistance due to the diversities in alloy compositions [2,21,42]. It is recognized that Cr-bearing MGs are able to be spontaneously passivated in air or other corrosive environments [21,43], and increasing Cr content within a certain limit can improve the corrosion resistance of Fe- or Ni-based MGs [24,31,35]. So far, however, little work has been done on the corrosion behavior of the BMGs with Cr content higher than 30 at.%. Consequently, the beneficial effect of Cr on the corrosion resistance

\* Corresponding author.

E-mail address: [xdhui@ustb.edu.cn](mailto:xdhui@ustb.edu.cn) (X.H. Hui).

may be confined. Recently, Xu et al. [44] reported a kind of Cr-rich  $\text{Cr}_x\text{Fe}_{58.8-x}\text{Mo}_{14.7}\text{C}_{14.7}\text{B}_{9.8}\text{Y}_2$  BMGs with high corrosion resistance in 1 M HCl. They found that the corrosion resistance was not significantly improved with further increasing Cr content, and considered that the threshold value of Cr content is around 29.4 at.% for the BMGs to achieve high corrosion resistance.

Very recently, the authors reported a new kind of Cr-Co-Nb-B BMGs with ultrahigh hardness and Young's moduli [45], which are promising to be used as wear resistant materials. However, the corrosion behavior and corrosion mechanism for this kind of Cr-based BMGs have not been concerned to date. In consideration of their possible applications for the pipeline anticorrosion, earth excavating, shipping and power-station industries, etc., it is imperative to characterize the corrosion properties of this kind of BMGs and figure out the influence mechanism of components on the corrosion resistance. In this work, two Cr-based BMGs were synthesized by copper-mold suction casting method. The corrosion resistance of Cr-based BMGs in HCl solutions was evaluated by immersion tests and electrochemical measurements. The compositions and evolution of passive films were investigated by X-ray photoelectron spectroscopy (XPS) tests. The corrosion resistance mechanism for the BMGs is discussed in detail.

## 2. Experimental

Cr-based BMGs with nominal compositions of  $\text{Cr}_{40}\text{Co}_{39}\text{Nb}_7\text{B}_{14}$  and  $\text{Cr}_{50}\text{Co}_{29}\text{Nb}_7\text{B}_{14}$  (for convenience, these two BMGs are denoted as Cr40 and Cr50 in the following context) were investigated. Alloy ingots were prepared by arc melting pure Cr (99.5%), Co (99.9%), B (99.5%), and Nb (99.9%) in a Ti-gettered pure argon atmosphere. Bulk cylindrical alloy samples with the diameter of 1–1.5 mm and length of about 25 mm were prepared by copper-mold suction casting method. The densities of these alloys were measured by the Archimedian method. The structure of these solidified rod specimens was examined by X-ray diffraction (XRD) using Mo  $K\alpha$  radiation. The thermal properties of these BMGs were investigated by using a differential scanning calorimeter (DSC) at a heating rate of 20 K/min.

The corrosion properties of these BMGs with the diameter of 1 mm were evaluated by immersion tests and electrochemical measurements. The cylindrical specimens were cut into about 12 mm in length. Prior to the immersion tests, the cross sections of all specimens were ground through successive grades of SiC paper up to 2000 grade, then the specimens were ultrasonically cleaned in deionized water for 5 min, ultrasonically degreased in acetone for 5 min, dried and exposed in air for 24 h. The weights of the specimens were measured using a special analytical balance in a DSC (Netzsch STA 449C) with a reliable precision of 1  $\mu\text{g}$ . The weight of each sample was measured for 3 times and the average was taken. The corrosion rates of these Cr-based BMGs were estimated from the weight loss after immersion in HCl solutions open to air at 298 K for 168 h. Scanning electron microscopy (SEM) was employed to examine the morphological features of BMG samples.

The electrochemical measurements were conducted in a three-electrode cell using a platinum counter electrode and a saturated calomel electrode (SCE). The polarization curves were measured with a potential sweep rate of 60 mV/min at 298 K. Prior to electrochemical measurements, the specimen ends were ground through successive grades of SiC paper up to 2000 grade, polished by using 2  $\mu\text{m}$  diamond suspension, ultrasonically cleaned in deionized water and dried in air. The electrolytes used in this work were 1, 3 and 6 M HCl solutions, which were prepared from reagent grade chemical and distilled water. For the measurement in 3 M HCl solution, two groups of specimens were exposed in air for 4 and 12 h after mechanical polishing, respectively. The specimens

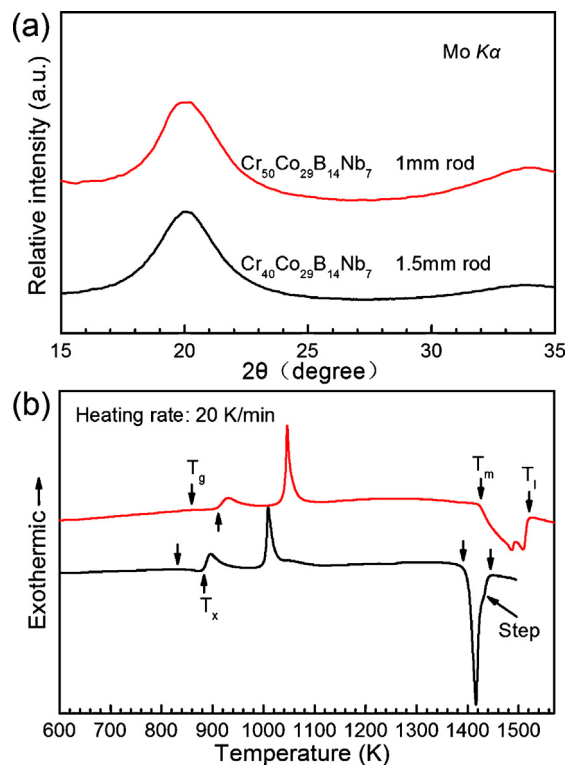


Fig. 1. (a) XRD patterns of as-cast Cr40 and Cr50 rods; (b) DSC curves of Cr40 and Cr50 BMGs.

were tested after they were immersed in 1 and 6 M HCl solutions for 0.5 h, and in 3 M HCl for 0.5, 2.5 and 4 h, respectively. It should be noted here that the immersion time mentioned in electrochemical tests represents the time that the specimens were stabilized in HCl solutions. All electrochemical measurements were performed at least twice for each specimen to confirm reproducibility.

X-ray photoelectron spectroscopy (XPS) measurements were performed by using a photoelectron spectrometer with Al- $K\alpha$  excitation ( $h\nu = 1486.8$  eV). The as-cast samples were exposed in air for at least 24 h, and the other samples were immersed in 1 or 3 M HCl for 168 h. The binding energies were calibrated by using carbon contamination with C 1s peak value of 284.8 eV. Photoelectron signal collecting areas were chosen at the smooth lateral faces of the cylindrical specimens.

## 3. Results and discussion

### 3.1. Glass formation and thermal properties of Cr-based BMGs

The XRD patterns of Cr40 and Cr50 alloy rods with 1 and 1.5 mm in diameter, respectively, are shown in Fig. 1(a). It is found that the two patterns exhibit almost identical shape of halo peaks. No crystalline diffraction peak is observed, indicating that the amorphous structure is formed for each alloy. The DSC curves of these BMGs with the critical diameters are shown in Fig. 1(b). Both of the DSC curves exhibit the glass transition and crystallization events, further confirming the amorphous feature of the structure. As shown in Fig. 1(b), the melting behavior of Cr40 alloy is significantly different from that of Cr50 alloy. The composition of Cr40 alloy is much close to a eutectic composition, although a tiny step can be observed on the melting peak. Actually, the difference in the melting behavior usually reflects the distinction in GFA of these BMGs [46].

The thermal parameters, including glass transition temperature  $T_g$ , onset temperature of crystallization  $T_x$ , supercooled liquid region,  $\Delta T_x (=T_x - T_g)$ , melting temperature  $T_m$ , liquid temperature

Download English Version:

<https://daneshyari.com/en/article/7894504>

Download Persian Version:

<https://daneshyari.com/article/7894504>

[Daneshyari.com](https://daneshyari.com)